J Therm Anal Calorim (2012) 108:939–946
DOI 10.1007/s10973-012-2381-8

Thermal and spectral properties and induction period, interfacial energy and nucleation parameters of solution grown anthracene

P. AnbuSrinivasan · G. Madhurambal · S. C. Mojumdar

CTAS2011 Conference Special Chapter

Abstract Anthracene crystals were grown by solution growth technique by adopting slow evaporation method from the solvents CS_2, CCl_4 and $CHCl_3$. The induction period was measured at various super saturations, and hence the interfacial energies were evaluated. Using the interfacial tension value, the nucleation parameters such as radius of the critical nuclei (r^*), the Gibbs free energy change for the formation of a critical nucleus (ΔG^*) and the number of molecules in the critical nucleus (i^*) were also calculated for all these solvents at two different temperatures. The effect of surface tension, viscosity and density of these solvents are correlated with interfacial tension. The solution grown crystals were subjected to UV, FTIR, NMR and X-ray diffraction studies. The purity and high-thermal stability of the grown crystals were determined using thermal analysis.

P. AnbuSrinivasan
Department of Chemistry, AVC College, Mayiladuthurai, Tamil Nadu, India

G. Madhurambal
Department of Chemistry, ADM College, Nagapattinam, Tamil Nadu, India

S. C. Mojumdar (✉)
Department of Chemistry, University of Guelph, Guelph, ON, Canada
e-mail: scmojumdar@yahoo.com

S. C. Mojumdar
Department of Chemical Technologies and Environment, Faculty of Industrial Technologies, Trenčín University of A. Dubček, 020 32 Púchov, Slovakia

Keywords Anthracene · Induction period · Interfacial energy · Nucleation parameters · Spectral characterization · Thermal studies

Introduction

The non-linear optical (NLO) properties of large organic molecules and polymers have been the subject of extensive theoretical and experimental investigations during the past two decades, and they have been investigated widely due to their high-NLO properties, rapid response in electro-optic effect and large second- or third-order hyperpolarizibilities compared to inorganic NLO materials [1]. Anthracene is one of the organic molecular crystals, which exhibits peculiar optical and electronic properties. It forms colourless monoclinic prismatic crystals with melting point 216 °C. The gel-aided solution method [2] was used to grow bigger and better quality crystals of anthracene at ambient temperatures.

The scintillation property of anthracene grown from Double Run Selective Self-seeding Vertical Bridgman technique (DRSSVBT) was studied [3]. Anthracene crystals were also grown using sublimation growth and Czochralski growth by Karl [4]. Anthracene crystals were grown from vertical Bridgmann technique by Chakkaravarthi [5]. Anthracene crystals were also grown from the solutions of benzene and n-pentane and from the vapour phase. Recently, we reported the growth of high-quality anthracene crystals by a simple solution technique [6]. Metastable zone width is an essential parameter for the growth of good crystals from solution, since it is the direct measure of the stability of the solution in its super saturated region [7]. Thermal, spectral and X-ray analyses are very useful techniques for material characterization [8–42]. In the present study, the growth and the metastable zone width of anthracene in CS_2, $CHCl_3$ and CCl_4 as solvents were determined. Various thermal, spectral and X-ray analyses were also used to characterize solution grown anthracene. The nucleation parameters of solution grown anthracene were determined using the interfacial tension and reported for the first time.

Experimental

Crystal growth

The anthracene used to grow crystals from solution was blue fluorescent grade. This anthracene was further purified by re-crystallization from carbon tetra chloride for several times. The final crystal was taken for growth.

Solubility of anthracene in CS_2, CCl_4 and $CHCl_3$ at various temperatures was determined. The solvents used were analar grade. Solubility determination shows that the solubility increases with temperature. This is shown by the solubility curves of anthracene in CS_2, CCl_4 and $CHCl_3$ in Figs. 1, 2 and 3, respectively.

Measurements

Powder X-ray diffractometry (XRD) analysis was performed with a graphite monochromated Cu K_α radiation.

FT-IR spectra were recorded using an AVATAR 330 FT-IR by KBr pellet technique in the range 400–4000 cm^{-1}.

UV–Visible absorption spectra were recorded using a Hitachi UV–VIS spectrophotometer in the spectral range 250–1200 nm.

The thermogravimetric (TG) and differential thermal analysis (DTA) were carried out using a NETZSCH STA 409C thermal analyzer in nitrogen atmosphere. The sample was heated between 30 and 550 °C at a heating rate of 10 °C/min.

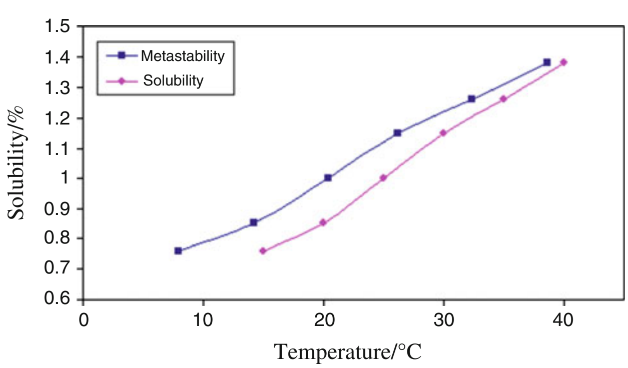

Fig. 1 Solubility and metastability of anthracene in CS_2

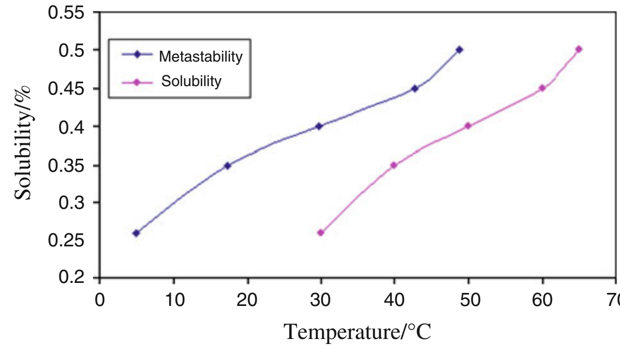

Fig. 2 Solubility and metastability of anthracene in CCl_4

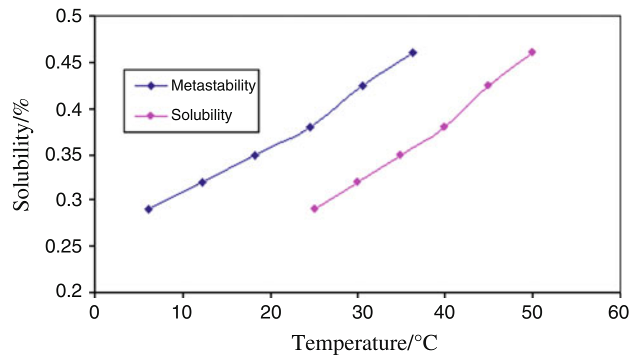

Fig. 3 Solubility and metastability of anthracene in $CHCl_3$

The NMR spectrum of solution grown anthracene was recorded using JEOL instrument, model GSX400, using $CDCl_3$ as solvent.

Determination of metastable zone width

Metastable zone width is an essential parameter for the growth of good crystals from solution, since it is the direct measure of the stability of the solution in its supersaturated region. After solubility determination, the metastable zone width of anthracene in CS_2, CCl_4 and $CHCl_3$ was determined. Saturated solutions of anthracene in these solvents at different temperatures were allowed for systematic slow cooling. The temperature at which the first nucleation was observed corresponds to their width of metastable zones. The metastable zone widths of anthracene in CS_2, CCl_4 and $CHCl_3$ are shown in Figs. 1, 2 and 3, respectively. The differences in metastable zone width of anthracene in CS_2, CCl_4 and $CHCl_3$ at various temperatures (30, 35 and 40 °C) are shown in Table 1. An important behaviour noted that the metastable zone width depends on solvent nature. At a particular temperature, the enhancement of metastable zone width is from CS_2 to $CHCl_3$ and from $CHCl_3$ to CCl_4. That is, larger metastable zone width is observed in CCl_4 than in $CHCl_3$ and CS_2. After solubility and metastable zone width determination, the saturated

Table 1 Comparison of metastable zone widths in various solvents

Temperature/°C	Solvents		
	CS_2	$CHCl_3$	CCl_4
30	3.8	17.7	25.1
35	2.6	16.8	24.2
40	1.4	15.5	22.8

solutions of anthracene were allowed for slow evaporation in room temperature. The crystals of different morphology were obtained in 1 or 2 days. The crystals were carefully harvested and subjected to characterization studies, viz., UV, NMR, FTIR, XRD and TG–DTA.

Induction periods and interfacial energies

There are several methods of measuring the induction period depending upon the solubility of the materials. Here the visual observation method was followed. Solutions of anthracene in CS_2 at different super saturation values were prepared and subjected to systematic slow evaporation. The time period that elapses between the achievement of super saturation and appearance of visible nuclei is taken as the induction period (t). Several trial runs were performed to minimize the error. Experiments were repeated for super saturation(s) like 1.10, 1.15 and 1.20 at two different temperatures. From the results obtained, a plot of ln t against $1/(\ln s)^2$ is drawn and is shown in Fig. 4. The interfacial tension was calculated from the slope of the curves using the equation

$$\ln t = \ln A + 16\pi\gamma^3 V^2 N / 3RT(\ln s)^2$$

where A is a constant related to the pre-exponential factor of the nucleation rate expression, V is the molar volume, N is the Avagadro number and R is the gas constant. The factor $16\pi/3$ in the above equation refers to the spherical nuclei. The interfacial tension between the anthracene and CS_2 is calculated by measuring the slope value of the curve obtained at the two temperatures.

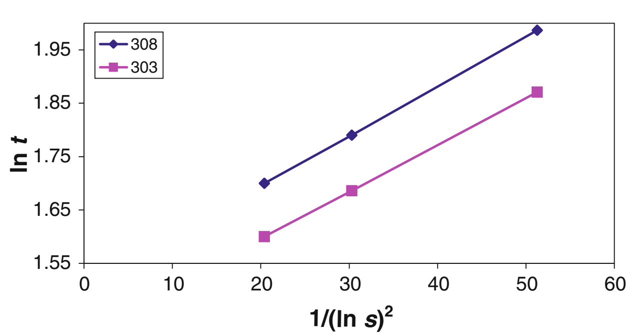

Fig. 4 A plot of ln t vs. $(1/\ln s)^2$ for anthracene grown from CS_2 at 303 and 308 K

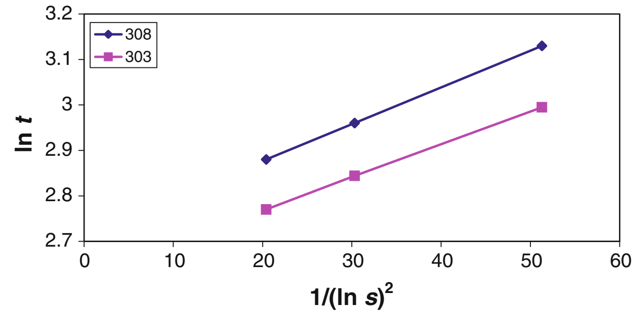

Fig. 5 A plot of ln t vs. $1/(\ln s)^2$ for anthracene grown from CCl_4 at 303 and 308 K

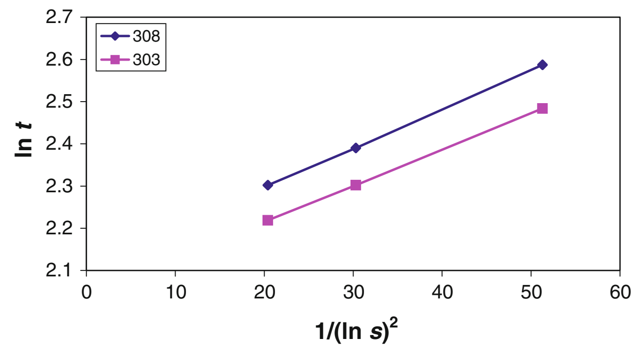

Fig. 6 A plot of ln t vs. $1/(\ln s)^2$ for anthracene grown from $CHCl_3$ at 303 and 308 K

Similar experiments were made in the case of CCl_4 and $CHCl_3$ solvents also. From the results obtained, plots of ln t against $1/(\ln s)^2$ are drawn and shown in Figs. 5 and 6. The effect of solvent and temperature on interfacial tension is presented in Table 2.

According to the classical homogenous nucleation theory, the Gibbs free energy required to form anthracene nucleus is given by

$$\Delta G = (4/3)\pi r^3 \Delta G_v + 4\pi r^2 \gamma \quad (2)$$

where ΔG_v is the Gibbs energy change per unit volume and r is radius of the nucleus. At the critical state, the free energy of formation obeys the condition that $d(\Delta G)/dr = 0$. Hence, the radius of the critical nucleus is expressed as

Table 2 Effect of temperature and solvent on interfacial tension

Solvent	Temperature/K	Slope value	Interfacial tension/mJ/m^2
CS_2	303	8.57×10^{-3}	1.230
	308	9.00×10^{-3}	1.257
$CHCl_3$	303	8.0×10^{-3}	1.202
	308	8.57×10^{-3}	1.230
CCl_4	303	7.5×10^{-3}	1.176
	308	8.10×10^{-3}	1.217

$$r^* = -2\gamma/\Delta G_v$$

where

$$\Delta G_v = -KT \ln s/V \tag{3}$$

where V is the molar volume and $s = C/C^*$, where C is the actual concentration and C^* is the equilibrium concentration.

Hence

$$r^* = 2v\gamma/KT \ln s \tag{4}$$

The critical Gibbs free energy is given by

$$\Delta G^* = 16\pi\gamma^3 v^2/\Delta G_v^2 \tag{5}$$

The number of molecules in the critical nucleus is expressed as

$$i^* = 4\pi(\gamma^*)^3/3V \tag{6}$$

Therefore, using the interfacial tension value, the radius of the critical nuclei (r^*), the Gibbs free energy change for the formation of a critical nucleus (ΔG^*) and the number of molecules in the critical nucleus (i^*) were calculated at two different temperatures for anthracene in CS_2 and presented in Table 3.

It was noted that with the increase in super saturation, the Gibbs free energy change for the formation of a critical nucleus (ΔG^*) decreases with radius (r^*). This favours the easy formation of nucleation in CS_2 solutions at higher super saturations.

Similar type of calculations used to calculate the nucleation parameters of anthracene in $CHCl_3$ and CCl_4, and the values are given in Tables 4 and 5, respectively.

Table 3 Nucleation parameters of anthracene crystal in CS_2

Super saturation ratio $S = C/C^*$	303 K			308 K		
	r^*/m	$(\Delta G^*)/10^{-15}$ kJ	i^* 10^{-10}	r^*/m	$(\Delta G^*)/10^{-15}$ kJ	i^* 10^{-10}
1.10	13.82	4.938	4.937	13.89	5.105	5.012
1.15	9.43	2.301	1.568	9.48	2.38	1.593
1.20	7.22	1.349	0.704	7.26	1.394	0.715

Table 4 Nucleation parameters of anthracene crystal in $CHCl_3$

Super saturation ratio $S = C/C^*$	303 K			308 K		
	r^*/m	$(\Delta G^*)/10^{-15}$ kJ	i^* 10^{-10}	r^*/m	$(\Delta G^*)/10^{-15}$ kJ	i^* 10^{-10}
1.10	13.50	4.609	4.602	13.60	4.938	4.70
1.15	9.21	2.147	1.461	9.28	2.301	1.49
1.20	7.05	1.259	0.655	7.10	1.348	0.669

Table 5 Nucleation parameters of anthracene crystal in CCl_4

Super saturation ratio $S = C/C^*$	303 K			308 K		
	r^*/m	$(\Delta G^*)/10^{-15}$ kJ	i^* 10^{-10}	r^*/m	$(\Delta G^*)/10^{-15}$ kJ	i^* 10^{-10}
1.10	13.21	4.323	4.311	13.45	4.639	4.551
1.15	9.00	2.014	1.363	9.18	2.163	1.447
1.20	6.90	1.181	0.614	7.03	1.267	0.649

Table 6 Effect of surface tension of solvents on interfacial tension

Solvent	Surface tension at 20 °C	Interfacial tension at 30 °C/mJ/m^2
CS_2	32.3	1.230
$CHCl_3$	27.14	1.202
CCl_4	27.0	1.176

The surface tension of the solvents CS_2, $CHCl_3$ and CCl_4 is in decreasing order. The effect of surface tension on interfacial tension is given in Table 6. The interfacial tension between the anthracene and CS_2, $CHCl_3$ and CCl_4 is also in decreasing order. The effect of viscosity of solvents on interfacial tension is given in Table 7. As viscosity increases, the interfacial tension decreases. The effect of density of solvents on interfacial tension is presented in Table 8. As density increases, the interfacial tension decreases.

UV spectral analysis

To analyse the transmission range and the suitability of solution grown anthracene crystals for optical applications, the UV–Visible spectrum was recorded and shown in Fig. 7. The spectrum shows the characteristic absorption of

Table 7 Effect of viscosity of solvents on interfacial tension

Solvent	Viscosity	Interfacial tension at 30 °C/mJ/m^2
CS_2	0.351	1.230
$CHCl_3$	0.518	1.202
CCl_4	0.845	1.176

Table 8 Effect of density of solvents on interfacial tension

Solvent	Density/g/mL	Interfacial tension at 30 °C/mJ/m^2
CS_2	1.2927	1.230
$CHCl_3$	1.4985	1.202
CCl_4	1.6320	1.176

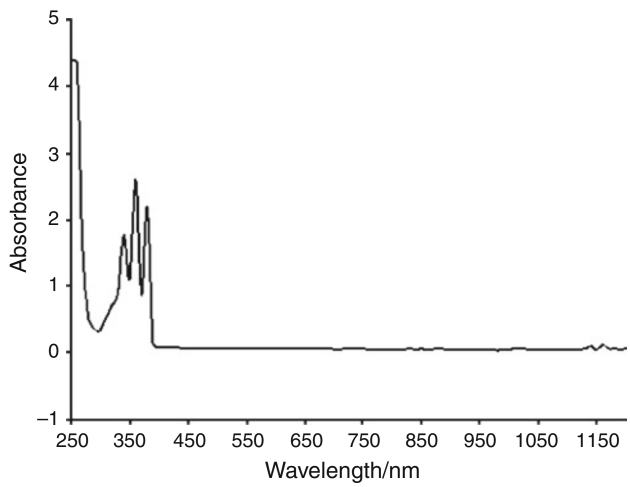

Fig. 7 UV spectrum of anthracene

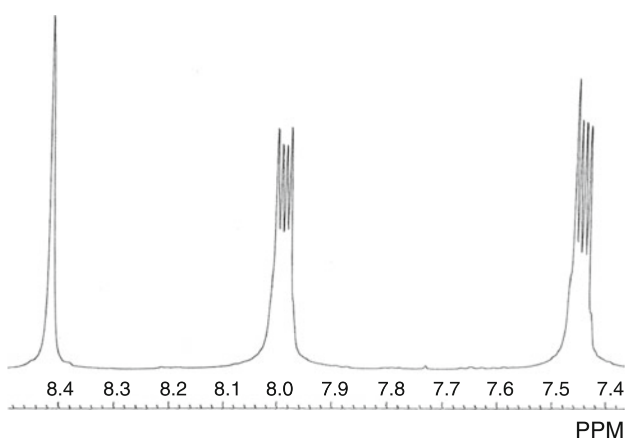

Fig. 8 Expanded [1]HNMR spectrum of solution grown anthracene

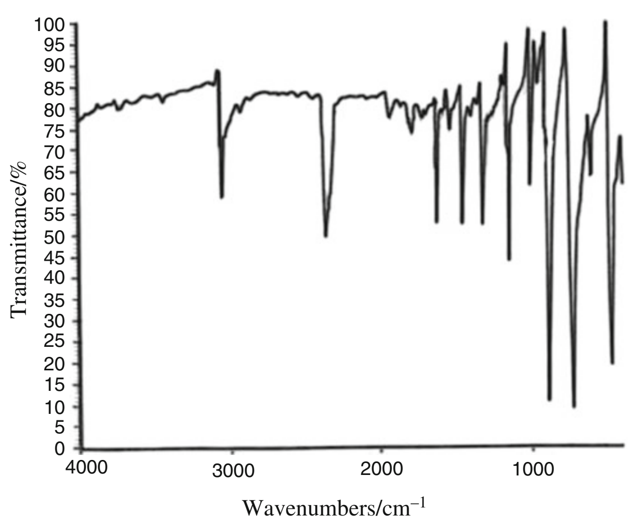

Fig. 9 FTIR spectrum of solution grown anthracene

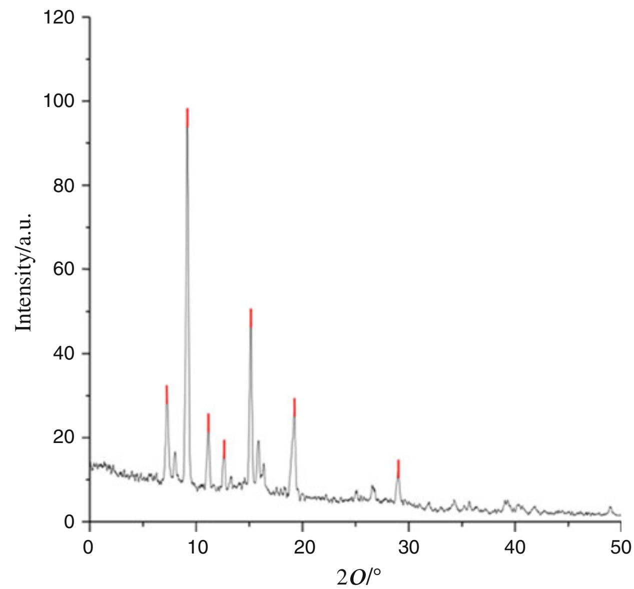

Fig. 10 XRD pattern of anthracene grown from CS_2

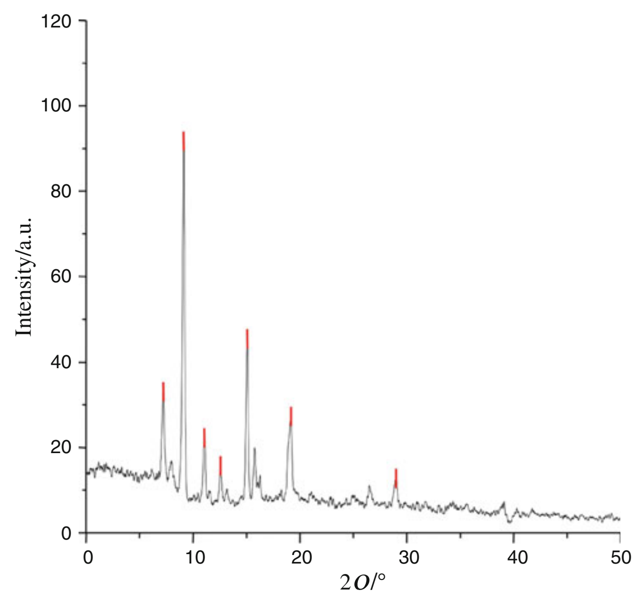

Fig. 11 XRD pattern of anthracene grown from CCl_4

anthracene between 300 and 400 nm which is assigned to aromatic ring. The UV spectrum proves the highly transparent nature of the material between 400 and 800 nm, which is one of the important requirements to a material for NLO applications.

NMR spectral studies

There are three sets of different kinds of protons present in anthracene molecule ($C_{14}H_{10}$). Therefore, we expect three

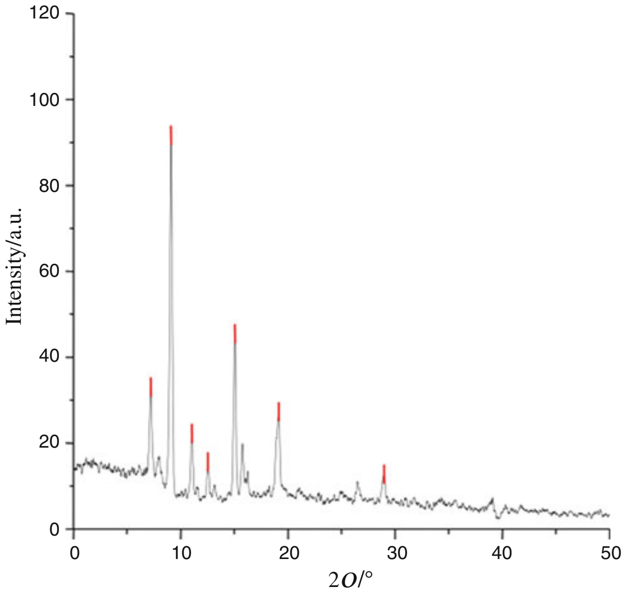

Fig. 12 XRD pattern of anthracene grown from $CHCl_3$

types of signals [43, 44]. The recorded ^{1}H NMR spectrum shown in Fig. 8 is well in accordance with theoretical spectrum. A singlet at 8.4 ppm is assigned to two protons. A double doublet at 8.0 ppm is assigned to four protons of one kind and another double doublet at 7.48 ppm is assigned to another kind of four protons.

FTIR spectral studies

The FTIR spectrum is an important record which gives sufficient information about the structure of a compound. The FTIR spectral studies were performed using the KBr pellet technique. The FTIR spectrum of anthracene grown form CS_2, $CHCl_3$ and CCl_4 is shown in Fig. 9. The middle of the IR spectrum of anthracene provides a characteristic peak due to aromatic C–H stretch at 3047 cm^{-1} which is very sharp. The sharpness of the peak shows that the hydrogen atoms in the anthracene ring are not exerting any bonding interaction with molecules. The skeletal vibrations (C=C bond) of the ring could be assigned to peaks 1619 and 1447 cm^{-1}. The presence of two sets of four adjacent hydrogen atoms is evidenced by the peak at 734.4 cm^{-1} due to C–H out of plane bending vibration.

The peak at 883 cm^{-1} is due to C–H out of plane bending vibration which corresponds to two isolated hydrogen atoms. Overtones or combination bands are found at 1926.7–1719.4 cm^{-1}. Out of plane (C=C bond) could be assigned to 469.3–438 cm^{-1} [43, 44].

X-ray diffraction studies

The powder X-ray diffraction studies were done, and lattice parameters were calculated. Most of the lattice parameters evaluated by powder X-ray diffraction studies of anthracene in CS_2 and CCl_4 as shown in Figs. 10, 11 and 12 are in good agreement with the Joint Committee on Powder Diffraction Standards (JCPDS) values. The prominent faces identified in the powder XRD pattern of anthracene grown from CS_2 are (1,0,0) $(\bar{1},1,0)$ (2,0,0) $(\bar{1},0,2)$ (2,0,2) which is shown in Fig. 10. The prominent faces identified in the XRD pattern of anthracene grown from CCl_4 and $CHCl_3$ are (1,0,0) (1,1,0) (0,1,1) (2,0,0) (1,0,2) (3,0,0) which is shown in Figs. 11 and 12. This reveals that the morphology of anthracene grown from different solvents is different.

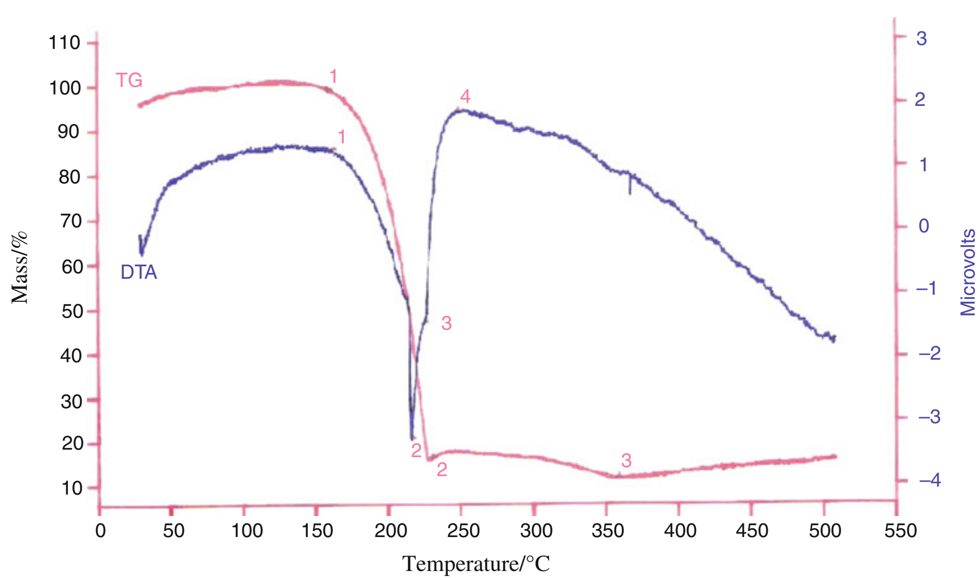

Fig. 13 TG and DTA curves of solution grown anthracene crystal

Thermal studies

TG and DTA were carried out on the crystal samples for qualitative analysis. The weight change in the sample with temperature was studied by TG, and the energy change in the sample with temperature was studied by DTA. The analysis was performed in nitrogen atmosphere.

The TG and DTA curves of anthracene grown from CS_2, CCl_4 and $CHCl_3$ given in Fig. 13 show the purity of the harvested anthracene crystals. The TG curve indicates that it is thermally stable up to 150 °C. Thermal studies show that the sharp exothermic peak (on DTA curve) corresponding to 216.40 °C indicate phase transition due to melting point, which exhibits the high purity of the grown crystals best and suitable for fabrication of best optical scintillator device.

Conclusions

The metastable zone width of anthracene in CS_2, CCl_4 and $CHCl_3$ solvents was determined for the first time. It was found that the metastable zone width depends on solvent nature. The effect of temperature and solvent on interfacial tension was determined. Using the interfacial tension value, the nucleation parameters such as radius of the critical nuclei (r^*), the free energy change for the formation of a critical nucleus (ΔG^*) and the number of molecules in the critical nucleus (i^*) were also calculated for all these solvents at two different temperatures. The effect of surface tension, viscosity and density of these solvents are correlated with interfacial tension. The UV spectrum proves the highly transparent nature of the material between 400 and 800 nm, which is one of the important requirements to a material for NLO applications. Thermal studies also support the purity of solution grown anthracene. All the characterization studies of solution grown anthracene are well in agreement with standard and theoretical value.

References

1. Bloembergen N. Nonlinear optics of polymers: fundamentals and applications. J Nonlinear Opt Phys Mater. 1996;15:1–7.
2. Babu KR, Deepa M, Nair CMK, Vaidyan VK. Growth of anthracene crystals by gel aided solution technique. Cryst Res Technol. 1998;33:817–9.
3. Chakkaravarthi AA, LakshmanaPerumal CK, Santhanaraghavan P, Sivaji K, Kumar P, Muralithar S, Ramasamy P. Preparation of high-quality anthracene crystals using double run selective self-seeding vertical Bridgman technique (DRSSVBT). J Cryst Growth. 2002;246:85–9.
4. Karl N. Growth and electrical properties of high purity organic molecular crystals. J Cryst Growth. 1990;99:1009–16.
5. Chakkaravarthi AA, LakshmanaPerumal CK, Santhanaraghavan PP, Jayavel P, Selvan R, Sivaji K, Gopalakrishnan R, Ramasamy P. Investigations on the growth of anthracene and *trans*-stilbene single crystals using vertical Bridgman technique. Mater Sci Eng. 2002;B95:236–41.
6. Madhurambal G, Anbusrinivasan P. Growth of high quality anthracene crystals by simple solution technique. Cryst Res Technol. 2006;41:231–5.
7. Boomadevi S, Dhanasekaran R, Ramasamy P. Investigations on nucleation and growth kinetics of urea crystals from methanol. Cryst Res Technol. 2002;37:159–68.
8. Czakis-Sulikowska D, Czylkowska A, Malinowska A. Thermal and other properties of new 4,4′-bipyridine-trichloroacetato complexes of Mn(II), Ni(II) and Zn(II). J Therm Anal Calorim. 2002;67:667–78.
9. Sawant SY, Verenkar VMS, Mojumdar SC. Preparation, thermal, XRD, chemical and FT-IR spectral analysis of $NiMn_2O_4$ nano particles and respective precursor. J Therm Anal Calorim. 2007;90: 669–72.
10. Mojumdar SC, Raki L. Preparation, thermal, spectral and microscopic studies of calcium silicate hydrate-poly(acrylic acid) nanocomposite materials. J Therm Anal Calorim. 2006;85: 99–105.
11. Sawant SY, Verenkar VMS, Mojumdar SC. Preparation, thermal, XRD, chemical and FT-IR spectral analysis of $NiMn_2O_4$ nanoparticles and respective precursor. J Therm Anal Calorim. 2007;90:669–72.
12. Porob RA, Khan SZ, Mojumdar SC, Verenkar VMS. Synthesis, TG, SDC and infrared spectral study of $NiMn_2(C_4H_4O_4)_36N_2H_4$—a precursor for $NiMn_2O_4$ nanoparticles. J Therm Anal Calorim. 2006;86:605–8.
13. Mojumdar SC, Varshney KG, Agrawal A. Hybrid fibrous ion exchange materials: past, present and future. Res J Chem Environ. 2006;10:89–103.
14. Doval M, Palou M, Mojumdar SC. Hydration behaviour of C2S and C2AS nanomaterials, synthesized by sol-gel method. J Therm Anal Calorim. 2006;86:595–9.
15. More A, Verenkar VMS, Mojumdar SC. Nickel ferrite nanoparticles synthesis from novel fumarato-hydrazinate precursor. J Therm Anal Calorim. 2008;94:63–7.
16. Varshney KG, Agrawal A, Mojumdar SC. Pyridine based thorium(IV) phosphate hybrid fibrous ion exchanger. Synthesis, characterization and thermal behaviour. J Therm Anal Calorim. 2007;90:721–4.
17. Madhurambal G, Ramasamy P, Anbusrinivasan P, Mojumdar SC. Thermal properties, induction period, interfacial energy and nucleation parameters of solution grown benzophenone. J Therm Anal Calorim. 2007;90:673–9.
18. Varshney G, Agrawal A, Mojumdar SC. Pyridine based cerium(IV) phosphate hybrid fibrous ion exchanger. Synthesis, characterization and thermal behaviour. J Therm Anal Calorim. 2007;90:731–4.
19. Mojumdar SC, Melnik M, Jona E. Thermal and spectral properties of Mg(II) and Cu(II) complexes with heterocyclic N-donor ligands. J Anal Appl Pyrolysis. 2000;53:149–60.
20. Borah B, Wood JL. Complex hydrogen bonded cations. The benzimidazole benzimidazolium cation. Can J Chem. 1976;50: 2470–81.
21. Mojumdar SC, Sain M, Prasad RC, Sun L, Venart JES. Selected thermo analytical methods and their applications from medicine to construction. J Therm Anal Calorim. 2007;60:653–62.
22. Mojumdar SC, Moresoli C, Simon LC, Legge RL. Edible wheat gluten (WG) protein films: preparation, thermal, mechanical and spectral properties. J Therm Anal Calorim. 2011;104:929–36.
23. Meenakshisundaram S, Parthiban S, Kalavathy R, Madhurambal G, Bhagavannarayana G, Mojumdar SC. Influence of organic

solvent on tristhioureazinc(II)sulphate crystals. J Therm Anal Calorim. 2009;96:125–9.
24. Gonsalves LR, Mojumdar SC, Verenkar VMS. Synthesis and characterisation of $Co_{0.8}Zn_{0.2}Fe_2O_4$ nanoparticles. J Therm Anal Calorim. 2011;104:869–73.
25. Rejitha KS, Mathew S. Investigations on the thermal behavior of hexaamminenickel(II) sulphate using TG-MS and TR-XRD. Glob J Anal Chem. 2010;1(1):100–8.
26. Pajtášová M, Ondrušová D, Jóna E, Mojumdar SC, Ľalíková S, Bazyláková T, Gregor M. Spectral and thermal characteristics of copper(II) carboxylates with fatty acid chains and their benzothiazole adducts. J Therm Anal Calorim. 2010;100:769–77.
27. Jóna E, Rudinská E, Sapietova M, Pajtášova M, Ondrušová D. Interactions of different heterocyclic compounds with monoionic forms of montmorillonite. I. Diffraction and spectral study of Co(II)-montmorillonite with 3- and 2-R pyridines (R = Me, Cl, NH2). Res J Chem Environ. 2006;10:31.
28. Kubranová M, Jóna E, Rudinská E, Nemčeková K, Ondrušová D, Pajtášová M. Thermal properties of Co-, Ni- and Cu-exchanged montmorillonite with 3-hydroxypyridine. J Therm Anal Calorim. 2003;74:251–7.
29. Jóna E, Hvastijová M, Kohout J. Thermal $N(CN)_2$-bridging reactions of dicyanamide complexes Ni{N(CN)2–2Ln in solid phase A: L = pyridine and its methyl derivatives. J Therm Anal Calorim. 1994;41:161–71.
30. Czakis-Sulikowska D, Czylkowska A. Complexes of Mn(II), Co(II), Ni(II) and Cu(II) with 4,4′-bipyridine and dichloroacetates. J Therm Anal Calorim. 2003;71:395–405.
31. Verma RK, Verma L, Ranjan M, Verma BP, Mojumdar SC. Thermal analysis of 2-oxocyclopentanedithiocarboxylato complexes of iron(iii), copper(ii) and zinc(ii) containing pyridine or morpholine as the second ligand. J Therm Anal Calorim. 2008; 94:27–31.
32. Anbusrinivasan P, Madhurambal G, Mojumdar SC. p-N,N dimethyl aminobenzaldehyde (DAB) grown by solution technique using CCl4 as growth medium—thermal studies and spectral characterization. J Therm Anal Calorim. 2009;96:111–5.
33. Ukraintseva EA, Logvinenko VA, Soldatov DV, Chingina TA. Thermal dissociation processes for clathrates $[CuPy_4(NO_3)_2]_2G$ (G = tetrahydrofurane, chloroform). J Therm Anal Calorim. 2004;75:337–45.
34. Mojumdar SC, Melník M, Jóna E. Thermoanalytical Investigation of Magnesium(II) Complexes with Pyridine as Bio-Active Ligand. J Therm Anal Calorim. 1999;56:541–6.
35. Rathore HS, Varshney G, Mojumdar SC, Saleh MT. Synthesis, characterization and fungicidal activity of zinc diethyldithiocarbamate and phosphate. J Therm Anal Calorim. 2007;90:681–6.
36. Mojumdar SC, Madhurambal G, Saleh MT. A study on synthesis and thermal, spectral and biological properties of carboxylato-Mg(II) and carboxylate-Cu(II) complexes with bioactive ligands. J Therm Anal Calorim. 2005;81:205–10.
37. Varshney KG, Agrawal A, Mojumdar SC. Pectin based cerium(IV) and thorium(IV) phosphates as novel hybrid fibrous ion exchangers. Synthesis, characterization and thermal behaviour. J Therm Anal Calorim. 2005;81:183–9.
38. Jona E, Rudinska E, Sapietova M, Pajtasova M, Ondrusova D, Jorik V, Mojumdar SC. Interaction of pyridine derivatives into the interlayer spaces of Cu(II)-montmorillonites. Res J Chem Environ. 2005;9:41–3.
39. Mojumdar SC, Miklovic J, Krutosikova A, Valigura D, Stewart JM. Furopyridines and furopyridine-Ni(II) complexes—synthesis, thermal and spectral characterization. J Therm Anal Calorim. 2005;81:211–5.
40. Mojumdar SC. Thermal properties, environmental deterioration and applications of macro-defect-free cements. Res J Chem Environ. 2005;9:23–7.
41. Madhurambal G, Mojumdar SC, Hariharan S, Ramasamy P. TG, DTC, FT-IR and Raman spectral analysis of Zna/Mgb ammonium sulfate mixed crystals. J Therm Anal Calorim. 2004;78: 125–33.
42. Mojumdar SC. Thermo analytical and IR spectroscopy investigation of Mg(II) complexes with heterocyclic ligands. J Therm Anal Calorim. 2001;64:629–36.
43. Kemp W. Organic spectroscopy. 3rd ed. New York: Wit Fireman; 1987.
44. Kalsi P. Spectroscopy of organic compounds. New Delhi: Wiley Eastern; 1985.